SUPPLEMENTAL DATA

Influence of physiologic folate deficiency on human papillomavirus type 16 (HPV16)-harboring human keratinocytes in vitro and in vivo.

Suhong Xiao[ζΨ], Ying-Sheng Tang[ζΨ], Rehana A. Khan[ζ], Yonghua Zhang[ζ], Praveen Kusumanchi[ζ‡], Sally P. Stabler[θ], Hiremagalur N. Jayaram[§‡], and Aśok C. Antony[ζ‡†]

From Departments of [ζ]Medicine, [§]Biochemistry & Molecular Biology, Indiana University School of Medicine, Indianapolis, Indiana; [θ]Department of Medicine, University of Colorado Health Sciences Center, Denver, Colorado, and [‡]Richard L. Roudebush Veterans Affairs Medical Center, Indianapolis, Indiana.

[Ψ] These authors contributed equally significant data to this paper

Materials—Restriction endonucleases, T4 DNA ligase, RNase A, RNase T1, proteinase K, RNase inhibitor, and the in vitro transcription kit were from Roche Molecular Biochemicals (Indianapolis, IN). All other chemicals of the highest analytical grade were from Sigma-Aldrich Inc. (St. Louis, MO). All oligodeoxynucleotides were synthesized by Invitrogen (San Diego, CA). Radiolabeled compounds were from Amersham Pharmacia Biotech (Piscataway, NJ).

Preparation of unlabeled L-homocysteine and purified recombinant glutathione S-transferase (GST)-hnRNP-E1 fusion protein—Unlabeled L-homocysteine was prepared from L-homocysteine thiolactone hydrochloride, purity over 99% (Sigma-Aldrich) and GST-hnRNP-E1 was prepared as described (1).

Determination if the RNA-protein interaction between the 3'-coding region of HPV16 L2 mRNA and hnRNP-E1 is responsive to homocysteine—Using primers 5'-ATA CAA GCT TCC AGT ACC AGC TAT ACC CTC-3' and 5'-CAC TGA ATT CCT AGG CAG CCA AAG AGA CAT-3' and plasmid PBR322/HPV16 (a gift from Professor Ann Roman, Indiana University) a new HPV16 L2 with a *Hin*dIII site in the 5' end and an *Eco*RI site in the 3' end was generated by PCR. The PCR product digested with *Hin*dIII and *Eco*RI was subcloned into a pSPT18 vector that was also linearized with *Hin*dIII and *Eco*RI to construct pSPT3'L2. The new plasmid was confirmed by restriction enzyme digestion and sequencing. The plasmid DNA was linearized with *Eco*RI and transcribed using the SP6/T7 Transcription Kit (1). Briefly, in vitro transcription was carried out at 37°C for 1 h in the presence of 100 μCi of [α-^{32}P]CTP and 1 mM of other three unlabeled nucleotides by T7 RNA polymerase. After transcription, template DNA was digested with DNase I (RNase-free) and RNA transcripts were purified using NucTrap Push columns. RNA-protein binding and gel-shift assays were carried out with 1 μg purified recombinant GST-hnRNP-E1 protein and [α-^{32}P]HPV16 L2 *cis*-element (1 x 10^5 cpm) in binding buffer (10 mM Hepes, pH 7.6, containing 3 mM $MgCl_2$, 40 mM KCl, 5% glycerol, 600 ng/μl yeast tRNA), and increasing physiological concentrations of L-homocysteine in a total volume of 15 μl. After incubation at 4˚C for 30 min, 1 μl of heparin (100 mg/ml) was added, and the sample was analyzed by PAGE followed by autoradiography overnight and densitometric analysis of the HPV16 L2 RNA-protein complexes (2,3).

In vitro transcription-translation of HPV16 L2 mRNA—A PCR was conducted using oligodeoxynucleotides L2FWD-*Nco*I (5'-GCA TCC ATG GAT GCG ACA CAA ACG TTC TGC-3') and L2RVS-*Xho*I (5'-ACT ACT CGA GGG CAG CCA AAG AGA CAT CTG-3') as primers and plasmid PBR322/HPV16 as template DNA. The PCR product digested with *Nco*I and *Xho*I was then subcloned into the pTriEx-4 Neo vector that was also linearized with *Nco*I and *Xho*I to construct pTriEx-4 Neo-L2. The new plasmid DNA was confirmed by restriction enzyme digestion and sequencing. To determine if binding of homocysteinylated-hnRNP-E1 to HPV16 L2 mRNA led to a direct effect in modulating HPV16 L2 protein synthesis during translation in vitro, we used the in vitro SP6/T7-

Transcription/Translation Kit. Although hnRNP-E1 is present in the reticulocyte lysate of commercial in vitro translation kits (4), there is an excess of β-mercaptoethanol (4.1 mM) that is also added, which significantly reduced the sensitivity of being able to detect any effect of physiologically-relevant [micromolar] concentrations of homocysteine on RNA-protein interactions. Accordingly, this excess reducing agent was quenched by the addition of N-ethyl maleimide. Briefly, after addition of DNA template (*Xho*I linearized pTriEx-4 Neo-L2 DNA) (0.5 μg/reaction) to the transcription mix, the reaction mixture was incubated at 30°C for 15 min. After adding 1 μl N-ethyl maleimide to a final concentration of 2 mM for 15 min, 1 μl L-homocysteine at various concentrations (0 to 100 μM), 8 μl of transcription-reaction and 1.6 μl [^{35}S]methionine were added to 38.4 μl of the translation-mix followed by incubation (1 h at 30°C). In other experiments, after adding (0.5 μg/reaction) DNA template (*Xho*I linearized pTriEx-4 Neo-L2 DNA) to the transcription mixture, and incubation at 30°C for 15 min, 1 μl of purified recombinant GST-hnRNP-E1 or bovine serum albumin (BSA) in various concentrations (0 to 1000 ng), 9 μl of transcription-reaction and 1.6 μl [^{35}S]methionine were added to 38.4 μl of translation-mixture followed by incubation for 1 h at 30°C. Two μl of translation-reaction was analyzed by 10% SDS-PAGE, autoradiography and densitometric analysis.

Total RNA was purified from the reaction mixtures using the GenElute Mammalian Total RNA Miniprep Kit (Sigma-Aldrich) followed by electrophoresis and photography to determine the potential for degradation of mRNA during the in vitro translation reaction.

Determination if HPV16 L2 single-stranded DNA binds to hnRNP-E1 in the presence of various concentrations of homocysteine—To prepare [[α-^{32}P]HPV16 L2 single-stranded DNA, the plasmid DNA (pTriEx-4 Neo-L2) was linearized with *Xho*I and extracted from agarose gel as template DNA. Forty cycles of PCR was carried out to produce [α-^{32}P]dCTP labeled single-stranded DNA of HPV16 L2 by using only one oligodeoxynucleotide (5'-GCA TCC ATG GAT GCG ACA CAA ACG TTC TGC-3') and 250 μCi of [α-^{32}P]dCTP and 1 mM of other three unlabeled deoxynucleotides. The PCR product was purified using the Quick Spin Columns (TE) kit (Roche) for radiolabeled DNA purification. Single-stranded DNA-protein binding and gel-shift assays were carried out with 1 μg dialyzed purified recombinant GST-hnRNP-E1 and 1 x 10^5 cpm of [α-^{32}P]HPV16 L2 single-stranded DNA in binding buffer and increasing concentrations of homocysteine (up to 100 μM) in a final volume of 15 μl. [α-^{32}P]CTP labeled HPV16 L2 RNA was used as a positive control to bind the same purified recombinant GST-hnRNP-E1. After incubation at room temperature for 30 min, 1 μl of heparin (100 mg/ml) was added and incubation was continued another 30 min. Electrophoresis of single-stranded DNA-Protein complexes was carried out using 6% native PAGE (60:1) and the dried gel autoradiographed at -80°C.

Quantitative RT-PCR (qRT-PCR), primers, and validation—Total RNA was extracted using the GenElute Mammalian Total RNA Miniprep kit and the manufacturer's instructions. Specific primers were designed to amplify HPV16 L1, L2, E6, E7 RNA using the online Invitrogen accelerate software. Fluorogenic labels for HPV16 *L1* were 5-carboxyfluorescein isothiocyanate-labeled 5'-CGG ATT GCG TGC AAC ATA TTC ATC*G-3', and 5'-GCC ACT GTC TAC TTG CCT CCT G-3'. Primers of HPV16 *L2* were 5-carboxyfluorescein isothiocyanate-labeled 5'-CTA CCA GAG GCT GCA TGT GAA GTG G*AG-3'. Primers for the human housekeeping gene, glyceraldehyde-3-phosphate dehydrogenase (*GAPDH*), were 6-carboxy-4',5'-dichloro-2'7'-dimethoxyfluorescein-labeled 5'-CAA CAG GAG GAG TGG GTG TCG CTG*TG -3' and 5'-GGC ATC CTG GGC TAC ACTGA-3'. Primers for HPV16 *E6* were 5-carboxyfluorescein isothiocyanate-labeled 5'-CAA CAG TAC CTC ACG TCG CAG TAA CTG*TG-3' and 5'-CAC AGG AGC GAC CCA GAA AGT-3'. Primers for HPV16 *E7* were 5-carboxyfluorescein isothiocyanate-labeled 5'-GAC CTG CCT AGT GTG CCC ATT AAC AGG*C-3' and 5'-CGG TTG TGC GTA CAA AGCA-3'. (An asterisk marks the position of the fluorogenic label in the sequences above). qRT-PCR was performed on a TaqMan ABI 7700 Sequence Detection System (PE Biosystems, Foster City, CA) using a SuperScript III Platinum One-Step qRT-PCR kit (Invitrogen, CA). Cycle conditions were as follows: after the first step for 15 min at 50°C and 10 min at 95°C, the samples were cycled 40 times at 95°C for 15 seconds and at 60°C for 60 seconds. For all quantitative analyses the comparative threshold cycle method [or relative standard curve method] was followed according to the

PE Biosystems instruction manual. All PCR reactions were performed in duplicate. Primers to GAPDH were run in parallel to standardize the input amount. Controls consisting of RNase free water were negative in all runs. Standard curves were subsequently developed using serial dilutions of total RNA extracted from (HPV16)BC-1-Ep/SL-*HF* cells (Supplemental Fig. S1). The purity of total RNA preparations was > 1.9 absorbance ratio at 260/280 nm. Serial dilutions of RNA for the standards ranged from 1 pg to 500,000 pg. Standard curves were developed for various RNA as well for GAPDH using the same serial dilutions of the (HPV16)BC-1-Ep/SL cell total RNA. This additional step facilitated relative quantification of unknown versus internal control.

Measurement of intracellular homocysteine in (HPV16)BC-1-Ep/SL cells—Intracellular thiols (cysteine, methionine, cystathionine, and homocysteine) were measured as described (3) with the following modifications to accommodate (HPV16)BC-1-Ep/SL cells which, unlike HeLa-IU_1 cells, could not tolerate centrifugation through silicone fluid, which resulted in significant loss of viability (5). In experiments in which increasing concentrations of homocysteine slowly accumulated in the growth media, we measured the amount of homocysteine that may have coated the surface of the culture plate after aspiration of excess extracellular media; this concentration needed to be quantified and subtracted from the total homocysteine concentration measured in cells at each time point. Accordingly, at each time point before cells were analyzed for intracellular homocysteine concentration, the spent growth medium was transferred to an empty plate and subsequently aspirated following which 1.8 ml D-PBS was then added to this plate and after mixing with the residual media, this sample was collected for analysis. The cells at each time point were then harvested in 1.8 ml of isotonic trypsin–EDTA (Gibco BRL) for 5 min at 37°C, and analyzed for cell number, protein and intracellular homocysteine (3).

Transient transfection of wild-type hnRNP-E1 into (HPV16)BC-1-Ep/SL cells—On the day before transfection, (HPV16)BC-1-Ep/SL-*HF* cells were trypsinized, counted, and plated in 6-well plates (2 ml of F-*HF* each well) at 2 x 10^6 cells per well to approximately 70-80% confluence on the day of transfection. For each well of cells to be co-transfected, 2 μg of pTriEx-neo DNA (pTriEx-neo/hnRNP-E1) with 2 μg of pCAT control DNA, and 10 μl of Lipofectamine 2000 reagent (Invitrogen) were diluted into 250 μl of Opti-MEM (Gibco). Once the Lipofectamine 2000 reagent was diluted it was combined with DNA in 250 μl of Opti-MEM and incubated at 22°C for 20 min to allow DNA-*LF*2000 reagent complexes to form. The DNA-Lipofectamine 2000 reagent complexes (500 μl) were then added directly to each well and mixed gently. Non-transfected (HPV16)BC-1-Ep/SL-*HF* cells were used as a background control whereas cells transfected with pCAT only were used as a control marker for transfection efficiency. After incubation at 37°C for 48 h, cells were harvested and divided into one part for CAT expression using CAT ELISA (Roche) to determine transfection efficiency, and another part for qRT-PCR analysis.

Determination if HPV16 57-nucleotide poly(T)-rich single-stranded DNA binds hnRNP-E1—The plasmid DNA pYS57 was linearized with *Hin*dIII and extracted from agarose gel as template DNA. Forty-cycles of PCR was carried out to produce [α-^{32}P]dTTP labeled single-stranded DNA of 57-nucleotide poly(T)-rich single-stranded DNA by using only one oligodeoxynucleotide (5'-TTT TTT CTT TTT TAT TTT CAT A -3') and 250 μCi of [α-^{32}P]dTTP and 1 mM of other three unlabeled deoxynucleotides. The PCR product was then purified with Quick Spin Columns (TE) (Roche). Single-stranded DNA-protein binding assays were carried out with 1 μg dialyzed purified recombinant GST-hnRNP-E1 protein and 1 x 10^5 cpm of [^{32}P]HPV16 57-nucleotide poly(T)-rich single-stranded DNA under similar conditions, as described above.

Interaction of endogenous homocysteinylated-hnRNP-E1 with the HPV16 57-nucleotide poly(U)-rich cis-element within cells and effects on downstream CAT reporter signal—To construct a plasmid containing the HPV16 57-nucleotide plasmid DNA placed proximal to a chloramphenicol acetyltransferase (CAT) reporter gene, a 236-bp intron from the pCAT3 control vector (Promega) was replaced with a 115-bp fragment of the 5'-untranslated region of HPV16 L2 cDNA containing the 57-nucleotide *cis*-element at

the *Hin*dIII and *NcoI* sites. Briefly, two oligonucleotides (5'-GTA CAA GCT TGT TAC ATA TAA TTG TTG T-3' and 5'-ACG TCC ATG GTG TTA AGT AAT AAC AGT TTA-3') were used as primers and HPV16 plasmid DNA was used as template to conduct the PCR reaction. The PCR product was linearized with *Hin*dIII and *Nco*I followed by subcloning into pCAT3 DNA digested with *Hin*dIII and *Nco*I to place the HPV16 57-nucleotide *cis*-element proximal to the CAT reporter gene [57nt+CAT]. pCAT control DNA and [57nt+CAT] plasmid DNA were purified by the endotoxin-free plasmid purification kit (Qiagen) and co-transfected into (HPV16)BC-1-Ep/SL-*HF* and (HPV16)BC-1-Ep/SL-*LF* cells (at 70-80% confluence) together with pSV-β-gal using Lipofectamine 2000 (Invitrogen). pSV-β-gal was employed as an internal control to determine the transfection efficiency using a chemi-luminescent assay (Roche). CAT activity of the transfected cells was determined using the CAT ELISA kit (Roche). The data of non-transfected cells were used as background and subtracted from the data of transfected cells. All data were normalized by transfection efficiency and protein concentration of each sample.

Specific binding between hnRNP-E1 and various mutations of HPV16 57-nucleotide RNA cis-element— The pWT, pM1, pM2, pM3, and pM4 plasmid DNAs were generated by subcloning annealed paired oligonucleotides (Fig. 3*D*) into pSPT19 digested with *Eco*RI and *Hin*dIII. All new constructed plasmid DNAs were purified using the High Pure Plasmid Isolation Kit (Roche) and the desired mutation was verified by sequencing. pWT, pM1, pM2, or pM3 plasmid DNA were then linearized by *Hin*dIII, and radiolabeled with [α-^{32}P]UTP during transcription and purified as described above. Gel-shift assays between hnRNP-E1 and [α-^{32}P]-labeled various wild-type and mutated HPV16 57-nucleotide RNA *cis*-elements were carried out in the absence or presence of 50 μM L-homocysteine, as described above.

Capture of intracellular HPV16 57-nucleotide RNA□hnRNP-E1 complexes formed in response to L-homocysteine by Slot-Blot Analysis—(HPV16)BC-1-Ep/SL-*HF* cells were cultured overnight to approximately 70-80% confluence in 100 mm plates (using 20 plates for each concentration) and treated for 2 h in F-*HF* medium containing L-homocysteine at various concentrations (0-, 12.5-, 25-, 50- μM) after which RNA-protein complexes were captured using the approach recently described (1). Briefly, plates were then irradiated once at 120 mJ/cm^2 using the UV Stratalinker 1800 (Stratagene) and after S-100 proteins were extracted (2), the UV-cross-linked RNA-protein complexes were specifically immunoprecipitated by anti-hnRNP-E1 antiserum (1). After incubation for 2 h and centrifugation at 13,600 x *g* for 5 min at 4°C, the pellets were treated with 100 ml of RNase A (dilution 1:5000) for 15 min, washed with 1 ml of buffer A, and resuspended in 0.2 ml of Proteinase K (4 mg/ml) followed by incubation at 37°C for 18 h on a shaking platform. After extraction of small RNA using the PureLink miRNA Isolation Kit (Invitrogen), the final concentration of RNA was determined using a nanoDrop ND1000 spectrophotometer (Thermo Fisher Scientific, Wilmington, DE). The RNAs were transferred to nylon membranes using a Hybri-Slot manifold (BRL Life Technologies) followed by probing with [^{35}S]labeled antisense [or control sense] probes to the HPV16 57-nucleotide RNA *cis*-element.

Effects of L-homocysteine on various CAT reporter constructs transfected into (HPV16)BC-1-Ep/SL HF cells—Following transient transfection of pCAT control or [57nt+CAT] plasmid DNAs into (HPV16)BC-1-Ep/SL-*HF* cells, these cells were incubated with various physiological concentrations of L-homocysteine and CAT mRNA and CAT activity was assessed, as described (1). The mRNA of pCAT and of [57nt+CAT] was determined by qRT-PCR using 5-carboxyfluorescein isothiocyanate-labeled 5'-CGG AAT GAA TAC CAC GAC GAT TTC CG-3' and 5'-ACC GTA ACA CGC CAC ATC TTG-3' primers from Invitrogen. Protein was estimated by the BCA protein assay (Pierce). β-galactosidase activity was determined by the β-galactosidase chemiluminescent assay (Roche). The extent of ß-galactosidase activity served as an internal standard for transfection efficiency of pCAT into (HPV16)BC-1-Ep/SL-*HF* cells. All data were normalized by internal standard and protein content of each treatment.

Analysis of the rates of biosynthesis and degradation of HPV16 L2 and L1 mRNA transcripts in (HPV16)BC-1-Ep/SL-HF and (HPV16)BC-1-Ep/SL-LF cells by qRT-PCR—For degradation studies, cells were first synchronized in their cell cycles using the double thymidine block technique (6). Briefly, (HPV16)BC-1-Ep/SL-*HF* and (HPV16)BC-1-Ep/SL-*LF* cells were exposed to F-*HF* or F-*LF* media (both

media containing 2 mM thymidine), respectively, for 18 h. This was then followed by exposure to thymidine-free F-*HF* or F-*LF* media, respectively, for 9 h before re-exposure to the same media containing 2 mM thymidine for 17 h; this led to arrest of cells at the beginning of S phase. The (HPV16)BC-1-Ep/SL-*HF* and (HPV16)BC-1-Ep/SL-*LF* cells were finally washed twice with F-*HF* or F-*LF* media, respectively, and then re-plated in the same medium in the absence or presence of actinomycin D (5 μg/ml). The cells were then harvested at various times from time-zero to the 6-hour time point after release from the second thymidine block, and lysed for total RNA isolation prior to qRT-PCR. The internal control, GAPDH, presented a stable transcript over the time course of the experiments and allowed for normalization of L1 and L2 mRNA levels.

Analysis of the rate of protein biosynthesis and degradation of HPV16 L2, L1, hnRNP-E1, and GAPDH in (HPV16)BC-1-Ep/SL-HF cells or (HPV16)BC-1-Ep/SL-LF cells—The rates of biosynthesis and degradation of various proteins-of-interest were determined, as described (1,3). Briefly, to determine the rate of biosynthesis of various proteins-of-interest, cells were first starved of cysteine overnight using cysteine-free *HF* or F-*LF* medium, respectively. (HPV16)BC-1-Ep/SL-*HF* cells or (HPV16)BC-1-Ep/SL-*LF* cells were then pulsed with [^{35}S]cysteine (250 μCi) in 4 ml of cysteine-free F-*HF* or F-*LF*, respectively, for various times indicated (up to 4 h) at 37°C. Cells were then harvested with a plastic cell scraper into 10 ml D-PBS containing 20 mM EDTA and a cocktail of complete protease inhibitors (Roche). To determine the rates of degradation of various proteins-of-interest, cells were first starved of cysteine overnight using cysteine-free *HF* or F-*LF* medium, respectively. These cysteine-depleted cells were then pulsed with [^{35}S]cysteine (250 μCi) in 4 ml of cysteine-free F-*HF* or F-*LF* for 4 h at 37°C followed by chase with F-*HF* or F-*LF*, and cells were harvested at various times (0, 16, 24, and 48 h). The samples were then subjected to specific immunoprecipitation with various specific antisera, which included either anti-GAPDH, anti-hnRNP-E1, anti-HPV16 L1 or anti-HPV16 L2 antisera, as described (1,3). The pellets containing immunoprecipated [^{35}S]cysteine-labeled protein-of-interest (20 μl each) were finally resuspended in 0.48 ml D-PBS. An aliquot (200 μl) was mixed with 10 ml of counting cocktail and analyzed for radioactivity in a β-scintillation counter. The results were calculated based on the amount of [^{35}S] incorporated into each sample and converted to nmol/mg protein based on protein concentrations. The curve-fitting analyses of these data were determined by linear regression.

Source of Antibodies—The mouse monoclonal L1 antibody [(ab3199) (CAMVIR-1)] was from Abcam, TX. The HPV16 L2 polyclonal rabbit anti-peptide antibody was custom-generated by Invitrogen against a unique L2 peptide sequence: QTPSLIPIVPGSPQYT (from amino acid position 425 of 473). Antibodies to an epitope in hnRNP-E1 that was shared only with hnRNP-E2 (1), but not with other members of the hnRNP family, were prepared as described (4). Antibodies to filaggrin, keratin 10, and involucrin were from Lab Vision Corp. (Fremont, CA).

Tissue histology, immunohistochemistry, and fluorescence microscopy, Western blot analysis—Histological staining of tissues was carried out as described (7). For immunohistochemical staining of L1, E6 or filaggrin and involucrin in paraffin embedded samples, slides were incubated at 70°C for 1 hr, washed twice with xylene (deparaffinizing) and then rehydrated in ethanol from 100% to 70%. The sections were then microwaved for 20 min in 10 mM sodium citrate buffer (pH 6.0) for antigen retrieval. Endogenous peroxidase activity was suppressed by immersing sections in 0.3% hydrogen peroxide/methanol for 30 min at 22°C. After processing with the Vector blocking kit (Vector Laboratories, Burlingame, CA), tissues were blocked in 10% (v/v) normal goat serum in phosphate buffered saline for 60 min and then incubated with anti-L1 and anti-E6 or anti-filaggrin and anti-involucrin (in 2% normal goat serum) overnight at 4°C. Control sections were incubated with non-immune rabbit serum. After washing with D-PBS, sections were processed using a Vectastain Elite avidin-biotin peroxidase kit (Vector Laboratories) with diaminobenzidine as the substrate. Sections were washed in tap water, and then dehydrated in an ascending ethanol series, cleared in xylene, and mounted with permount (Fisher Scientific, Pittsburgh, PA). Images were captured with either a Leica MZ APO (Leica Microsystems, Heerbrugg, Switzerland) dissecting microscope or a Leitz DMLB light microscope equipped with a Diagnostic Instruments Spot digital camera (Diagnostic Instruments, Sterling, MI) and

processed using Adobe Photoshop software (San Jose, CA). Control experiments verified that specific immunostaining did not occur in the absence of primary antibodies.

Immunofluorescence for filaggrin protein was performed on 4 um sections from paraffin-embedded raft cultures as described (8). Briefly, the slides were deparaffinized with xylenes and rehydrated through a graded series of alcohols, following which the antigens were unmasked in sodium citrate buffer (10 mM at pH 6.0) for 20 min while rotating the specimens in the microwave. Sections were blocked with 2% horse serum (supplied in the Vectastain kit) in D-PBS for 60 min and then incubated overnight at 4°C with anti-filaggrin antibody at a 1:100 dilution in 2% blocking serum. The antigen-bound antibody was detected using Texas red-conjugated anti-mouse secondary antibody (Vector Laboratories) diluted 1:100 in D-PBS for 60 min at 22°C. The slides were then mounted with fluorescence mounting medium containing 4',6-diamidino-2-phenylindole (DAPI) (Vector laboratories), which stains nuclei blue, overnight at 4°C.

Western blot analysis (3) was carried out to determine the presence of HPV16-specific tumors on the primary and secondary tumors. Antiserum to human nicotinamide mononucleotide adenylyltransferase-2 (Santa Cruz Biotechnology, Santa Cruz, CA), which only gave a positive signal with HT29 (human colon cancer) cells, was used to confirm the specificity of the HPV16-signals using HPV16 antibodies.

Electron microscopic analysis of HPV16-organotypic rafts—The method of Clendenon et al was followed (9). Briefly, HPV16-organotypic rafts were fixed with 2% paraformaldehyde/2% glutaraldehyde 0.1 M cacodylate buffer at 4°C overnight. After rinsing in buffer, these rafts were postfixed with 1% osmium tetroxide in 0.1 M cacodylate buffer for 1 h, rinsed in buffer, and then dehydrated with ethyl alcohols from 50-100%. After dehydration, infiltration was initiated sequentially with changes in propylene oxide followed with a 1:1 mixture of propylene oxide and embedding media (Embed 812, Electron Microscopy Sciences, Fort Washington, PA) for 12-18 h, and then 100% embedding media for 6 h. After infiltration, rafts were embedded and polymerized at 60°C for 12-18 h. The raft blocks were sectioned at 70 nm with a diamond knife (Diatome/Electron Microscopy Sciences, Fort Washington, PA) using an Ultracut UCT ultramicrotome (Leica, Bannockburn, IL) and heavy metal stained with uranyl acetate. Sections were viewed on a Tecnai BioTwin transmission electron microscope (FEI, Hillsboro, OR). Digital images were taken with an AMT (Advanced Microscopy Techniques, Danvers, MA) CCD camera.

SUPPLEMENTAL REFERENCES

1. Tang, Y. S., Khan, R. A., Zhang, Y., Xiao, S., Wang, M., Hansen, D. K., Jayaram, H. N., and Antony, A. C. (2011) *J. Biol. Chem.* **286**, 39100–39115
2. Sun, X. L., and Antony, A. C. (1996) *J. Biol. Chem.* **271**, 25539-25547
3. Antony, A. C., Tang, Y.-S., Khan, R., Biju, M. P., Xiao, X., Li, Q.-J., Sun, X.-L., Jayaram, H. N., and Stabler, S. (2004) *J. Clin. Invest.* **113**, 285-301
4. Xiao, X., Tang, Y.-S., Mackins, J. Y., Sun, X.-L., Jayaram, H. N., Hansen, D. K., and Antony, A. C. (2001) *J. Biol. Chem.* **276**, 41510-41517
5. Sun, X. L., Murphy, B. R., Li, Q. J., Gullapalli, S., Mackins, J., Jayaram, H. N., Srivastava, A., and Antony, A. C. (1995) *J. Clin. Invest.* **96**, 1535-1547
6. Whitfield, M. L., Zheng, L. X., Baldwin, A., Ohta, T., Hurt, M. M., and Marzluff, W. F. (2000) *Mol. Cell. Biol. 20(12):4188-98*
7. Xiao, S., Hansen, D. K., Horsley, E. T., Tang, Y. S., Khan, R. A., Stabler, S. P., Jayaram, H. N., and Antony, A. C. (2005) *Birth Defects Res. A Clin. Mol. Teratol.* **73**, 6-28
8. Balsitis, S., Dick, F., Lee, D., Farrell, L., Hyde, R. K., Griep, A. E., Dyson, N., and Lambert, P. F. (2005) *J. Virol.* **79**, 11392-11402
9. Clendenon, S. G., Shah, B., Miller, C. A., Schmeisser, G., Walter, A., Gattone, V. H., 2nd, Barald, K. F., Liu, Q., and Marrs, J. A. (2009) *Dev. Dyn.* **238**, 1909-1922
10. Lyon, M., Rastan, S., and Brown, S. (1996) *Genetic Variants and Strains of the Laboratory Mouse*, Third ed., Oxford University Press, Oxford, UK

11. Waggie, K. S., Wu-Owens, J., Hollifield, V., and Hansen, C. T. (1992) *Lab. Anim. Sci.* **42**, 375-377
12. Shanice, V., Sheryl, J., Andrew, I., Craig, F., Beth, L., and Dale, M. (2010) *Proc. Amer. Assoc. Cancer Res.*, http://www.harlan.com/online_literature/scientific_posters_and_abstracts (April 17-21)
13. Yuspa, S. H., Kilkenny, A. E., Steinert, P. M., and Roop, D. R. (1989) *J. Cell Biol.* **109**, 1207-1217

Supplemental Table S1. Characteristics of immunodeficient mice used to implant day-18 HPV16-organotypic rafts developed in high- and low-folate medium.

(Data in the Table was obtained from Harlan; www.harlan.com)

Model	Nomenclature	Hair	T Cells	B Cells	NK Cells
Beige Nude XID	Hsd:NIHS-*Lyst^{bg} Foxn1^{nu}Btk^{xid}*	No	No	No	No
Athymic Nude	Hsd:Athymic Nude-*Foxn1^{nu}*	No	No	Yes	Yes
SHrN™ SCID	NOD.Cg-*prkdc^{scid}Hr^{hr}*/NCrHsd	No	No	No	Impaired

The Beige Nude XID (Hsd:NIHS-*Lyst^{bg} Foxn1^{nu}Btk^{xid}*) mouse is a T and B cell deficient due to thymic agenesis (lack of functional thymus to mature T cells) conferred by the *nu* mutation and the XID mutation, which results in lack of B cells due to defective B cell signaling. The *xid* defect is X-linked, so hemizygous males and homozygous females have a defective immune response to type 2 thymus-independent (TI-2) antigens, a normal response to type 1 thymus-independent antigens, an impaired immune response to thymus-dependent antigens, and lymphocytes with impaired response to B-cell mitogens. The *xid* defect is expressed in B-cells, which are characterized by low complement receptor (10). The *nu* mutation produces defects in cytotoxic T cells, macrophages, and polymorphonuclear leukocytes. The *bg* mutation produces impaired NK cell function, effectively preventing NK-mediated tumor cell lysis (11).

The Athymic Nude (Hsd:Athymic Nude-*Foxn1^{nu}*) mouse and all homozygous *nu/nu* mice exhibit a rudimentary thymus resulting in T-cell deficiency due to the autosomal recessive *Foxn1^{nu}* mutation on chromosome 11. Athymic mice are phenotypically hairless (although sparse hair growth is possible) and display normal B-cell function. Heterozygous, *Foxn1^{nu}/Foxn1^{+},* mice do not show partial expression of the *nu* phenotype (10).

The SHrN™ SCID (NOD.Cg-*prkdc^{scid}Hr^{hr}*/NCrHsd) mouse is a hairless triple-immunodeficient mouse. This model was developed by transferring the Prkdc^{scid} mutation onto the Non-Obese Diabetic (NOD) mouse background, resulting in a B and T cell deficiency, a functional deficit of NK cells, defective function of antigen-presenting cells, decreased cellular immune response in the spleen, suppressed leakiness compared to other SCID mice, loss of pelage around 10 days of age and complete hair loss around 5–6 weeks (12).

As shown in (Fig. 7, main text), an HPV16-*low folate*-organotypic raft, which exhibited high level (88%) integration of HPV16 DNA into genomic DNA, was transformed into an aggressive HPV16-oncogene expressing cancer within 12 weeks in one of two Beige Nude XID mice tested. Fragments of this primary tumor also developed into secondary aggressive malignancies within 2 weeks in all Beige Nude XID and Athymic Nude mice tested, and tumor fragments from these secondary tumors further developed into tertiary cancers in all SHrN™ SCID mice tested.

Supplemental Fig. S1. Quantitative RT-PCR (qRT-PCR) profiles with the standard curves for the target RNA HPV16 L1 (*A*) and HPV16 L2 (*C*) with accompanying reference RNA (GAPDH) (*B*) and (*C*), respectively*)* in (HPV16)BC-1-Ep/SL-*HF* cells. (*E*). qRT-PCR profiles for target RNA (HPV16 L1, L2, E6, E7, hnRNP-E1, and human folate receptor-α (hFR-α) in BC-1-Ep/SL cells that were devoid of the HPV16 genome. (*F*) qRT-PCR profiles for target RNA ([HPV16 L1, L2, E6, E7, hnRNP-E1, and hFR-α in (HPV16)BC-1-Ep/SL-*HF* cells which contained the HPV16 genome.

Standard curves were developed by using serial dilutions of total RNA extracted from (HPV16)BC-1-Ep/SL cells. The purity of total RNA preparations were > 1.9 absorbance ratio at 260/280 nm. Serial dilutions of RNA for the standards ranged from 1 pg to 500,000 pg. Standard curves were developed for various mRNA as well for the housekeeping gene GAPDH, using the same serial dilutions of the (HPV16)BC-1-Ep/SL-*HF* cell total RNA. This additional step facilitated relative quantification of unknown versus internal control.

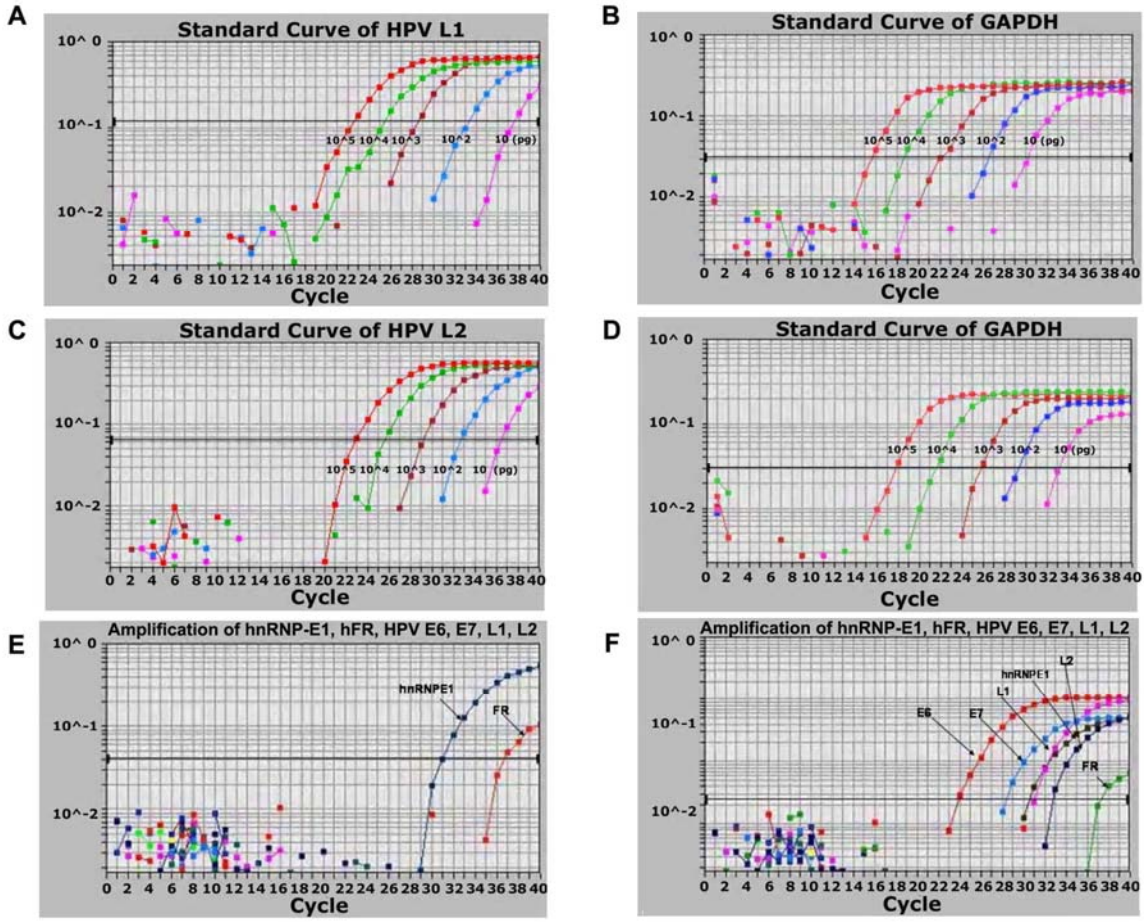

Supplemental Fig. S2. Analysis of the stability of HPV16 L2 RNA during in vitro translation. RNA from each of the reaction mixtures (shown in the Figure) following in vitro translation was extracted and analyzed on 1% agarose gels. There was no change in RNA with the addition of variables (N-ethylmaleimide, NEM; L-homocysteine or purified recombinant GST-hnRNP-E1).

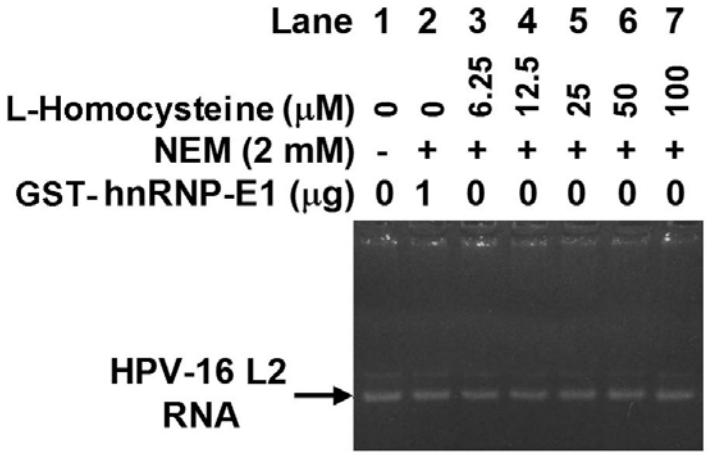

Supplemental Fig. S3. HPV16-*high folate*-organotypic rafts (*A,C,F,I*) and HPV16-*low folate*-organotypic rafts (*B,D,G,J*) that were developed from (HPV16)BC-1-Ep/SL cells in high-folate or physiologic low-folate conditions. Differentiation of rafts was confirmed by histology after hematoxylin-eosin staining which demonstrates differentiation in the superficial layer of these rafts (*A* and *B*); by immunofluorescence (*C* and *D*) with filaggrin—a filament-associated protein (stained in red) that binds to keratin fibers in epithelial cells and is a bona fide differentiation marker (13); by immunohistochemistry for keratin 10 (*F* and *G*) and filaggrin (*I* and *J*); and by Western blots of the HPV16-organotypic rafts, using the entire raft which was probed with anti-filaggrin and anti-keratin antibodies (*E* and *H*).

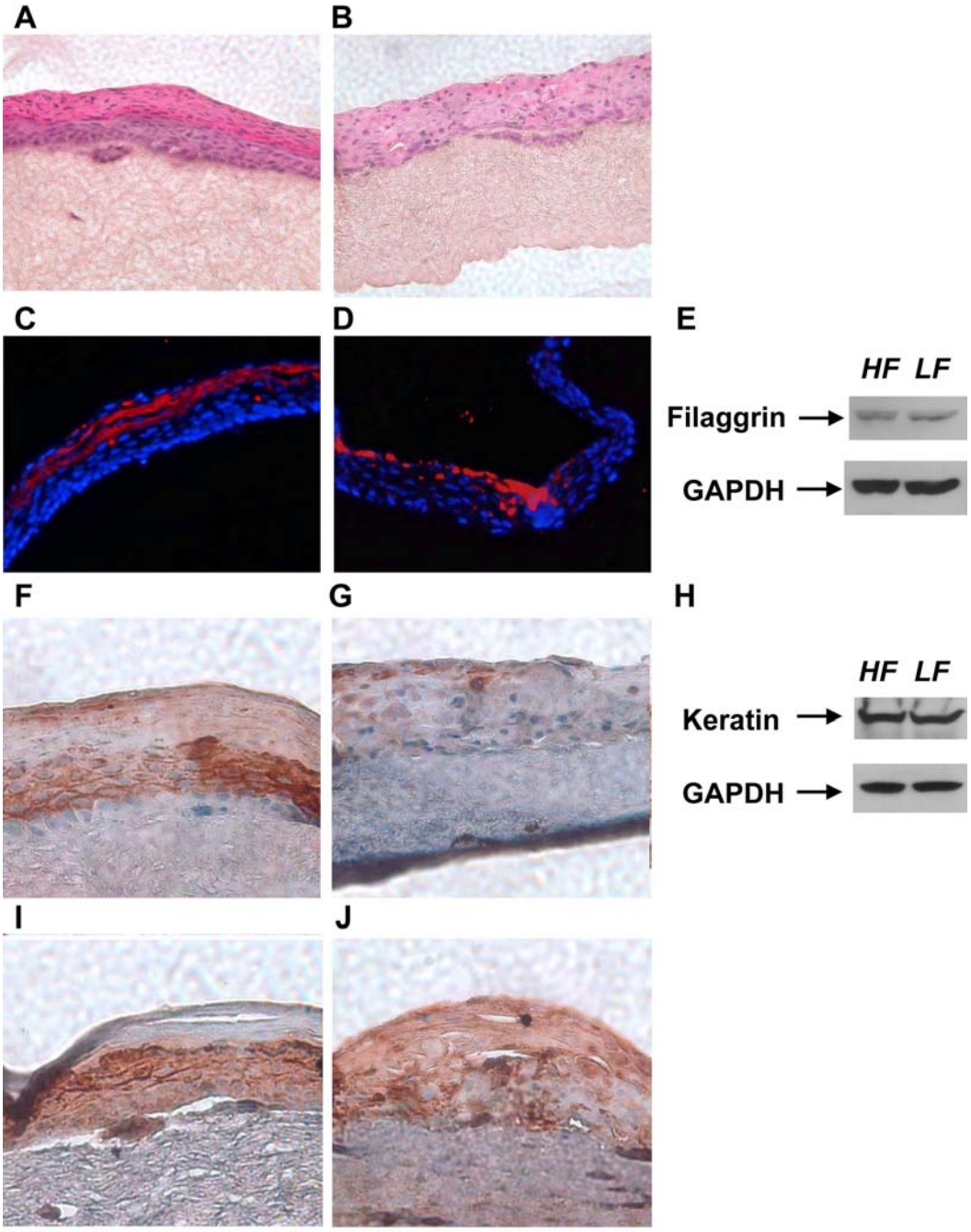

There were architectural abnormalities arising from disordered proliferation in HPV16-*low folate*-organotypic rafts when compared to HPV16-*high folate*-organotypic rafts. This feature was similar to the findings consistently noted in differentiated epithelial tissues from folate-deficient murine fetuses (7), where the differentiation of superficial keratinocytes was only minimally perturbed.